Heliyon 10 (2024) e29390

Contents lists available at ScienceDirect

Heliyon

journal homepage: www.cell.com/heliyon

Research article

Design, synthesis, biological and computational screening of novel pyridine-based thiadiazole derivatives as prospective anti-inflammatory agents

Naresh Podila [a], Naveen Kumar Penddinti [b], Mithun Rudrapal [a], Gourav Rakshit [c], Sathish Kumar Konidala [a,**], Veera Shakar Pulusu [d], Richie R. Bhandare [e,f,***], Afzal B. Shaik [g,h,*]

[a] *Department of Pharmaceutical Sciences, School of Biotechnology and Pharmaceutical Sciences, Vignan's Foundation for Science, Technology & Research, Vadlamudi, Guntur, 522213, Andhra Pradesh, India*
[b] *Vikas College of Pharmaceutical Sciences, Suryapet, Telangana, India*
[c] *Department of Pharmaceutical Sciences & Technology, Birla Institute of Technology, Mesra, India, Ranchi, 835215, Jharkhand, India*
[d] *Ohio University, Department of Chemistry & Biochemistry, Athens, OH, USA, 45701*
[e] *Department of Pharmaceutical Sciences, College of Pharmacy and Health Sciences, Ajman University, P O Box 346, Ajman, United Arab Emirates*
[f] *Centre of Medical and Bio-allied Health Sciences Research, Ajman University, P O Box 346, Ajman, United Arab Emirates*
[g] *St. Mary's College of Pharmacy, St. Mary's Group of Institutions Guntur, Affiliated to Jawaharlal Nehru Technological University Kakinada, Chebrolu, Guntur, 522212, Andhra Pradesh, India*
[h] *Center for Global Health Research, Saveetha Medical College, Saveetha Institute of Medical and Technical Sciences, India*

ARTICLE INFO

Keywords:
Acute toxicity
Anti-inflammatory activity
Cyclooxygenase-2
In silico studies
Pyridine derivatives
Thiadiazole derivatives

ABSTRACT

In this study, a novel series of pyridine-based thiadiazole derivatives (**NTD1-NTD5**) were synthesized as prospective anti-inflammatory agents by combining substituted carboxylic acid derivatives of 5-substituted-2-amino-1,3,4-thiadiazole with nicotinoyl isothiocyanate in the presence of acetone. The newly synthesized compounds were characterized by FTIR, ^{1}H NMR, ^{13}C NMR, and mass spectrometry. First, the compounds underwent rigorous *in vivo* testing for acute toxicity and anti-inflammatory activity and the results revealed that three compounds-**NTD1**, **NTD2**, and **NTD3**, displayed no acute toxicity and significant anti-inflammatory activity, surpassing the efficacy of the standard drug, diclofenac. Notably, **NTD3**, which featured benzoic acid substitution, emerged as the most potent anti-inflammatory agent among the screened compounds. To further validate these findings, an *in silico* docking study was carried out against COX-2 bound to diclofenac (PDB ID: 1pxx). The computational analysis demonstrated that **NTD2**, and **NTD3**, exhibited substantial binding affinity, with the lowest binding energies (−8.5 and −8.4, kcal/mol) compared to diclofenac (−8.4 kcal/mol). This alignment between *in vivo* and *in silico* data supported the robust anti-inflammatory potential of these derivatives. Moreover, molecular dynamics simulations were conducted, extending over 100 ns, to examine the dynamic

* Corresponding author. St. Mary's College of Pharmacy, St. Mary's Group of Institutions Guntur, Affiliated to Jawaharlal Nehru Technological University Kakinada, Chebrolu, Guntur, 522212, Andhra Pradesh, India.
** Corresponding author. Department of Pharmaceutical Sciences, School of Biotechnology and Pharmaceutical Sciences, Vignan's Foundation for Science, Technology & Research, Vadlamudi, Guntur, 522213, Andhra Pradesh, India.
*** Corresponding author. Department of Pharmaceutical Sciences, College of Pharmacy and Health Sciences, Ajman University, P O Box 346, Ajman, United Arab Emirates.
E-mail addresses: sathishkonidala@gmail.com (S.K. Konidala), r.bhandareh@ajman.ac.ae (R.R. Bhandare), bashafoye@gmail.com (A.B. Shaik).

https://doi.org/10.1016/j.heliyon.2024.e29390
Received 4 January 2024; Received in revised form 12 March 2024; Accepted 8 April 2024
Available online 9 April 2024

interactions between the ligands and the target protein. The results solidified **NTD3**'s position as a leading candidate, showing potent inhibitory activity through strong and sustained interactions, including stable hydrogen bond formations. This was further confirmed by RMSD values of 2-2.5 Å and 2-3Á, reinforcing **NTD3**'s potential as a useful anti-inflammatory agent. The drug likeness analysis of **NTD3** through SwissADME indicated that most of the predicted parameters including Lipinski rule were within acceptable limits. While these findings are promising, further research is necessary to elucidate the precise relationships between the chemical structures and their activity, as well as to understand the mechanisms underlying their pharmacological effects. This study lays the foundation for the development of novel anti-inflammatory therapeutics, potentially offering improved efficacy and safety profiles.

1. Introduction

Many chronic and acute diseases are characterized by inflammation, including autoimmune disorders (e.g., rheumatoid arthritis, lupus), cardiovascular diseases, neurodegenerative conditions (e.g., Alzheimer's disease), and various types of cancer [1]. Developing new anti-inflammatory drugs can provide more effective treatment options for these conditions, improving patients' quality of life and prognosis [2]. Existing anti-inflammatory drugs, such as nonsteroidal anti-inflammatory drugs (NSAIDs) and corticosteroids, can cause significant side effects like indigestion, dizziness, head ache, stomach ache, ulcers, diarrhoea, anaemia, osteoporosis, immunosuppression, psychological effects, glucose intolerance, cataracts, glaucoma and in rare cases lead to heart failure or attacks, kidney problem, and liver problems when used long-term [3–5]. Discovery and development of new biologically significant agents with improved safety profiles can reduce these side effects, making treatment more tolerable for patients. Advances in molecular biology and genetics have enabled researchers to identify specific inflammatory pathways and specific proteins or targets involved in causation of inflammation. New anti-inflammatory agents can be designed to target these specific pathways, offering more targeted and precise therapies while minimizing off-target effects ultimately minimises the side effects or adverse reactions [6]. Chronic inflammatory conditions often require long-term treatment. Developing new anti-inflammatory agents with better efficacy and tolerability can enhance disease management and reduce the need for frequent hospitalizations and interventions.

Privileged heterocyclic rings bearing nitrogen and sulfur atoms are indispensable tools in the quest to develop novel drugs including anti-inflammatory agents [7,8]. Numerous studies in scientific literature have indicated that synthetic compounds containing heterocyclic structures possess the capacity to mitigate acute and chronic inflammatory conditions, potentially promoting healing and relief. Their structural diversity, biological activity, target specificity, and clinical relevance make them valuable building blocks for creating effective and safer treatments for inflammatory conditions [9,10]. Among the others, medicinal chemists often use the pyridine and thiadiazole rings as scaffolds to build and modify molecules with desired pharmacological properties. This approach enables the development of novel drugs and the improvement of existing ones. Thus, these two rings had emerged as potential heteroaryl rings of interest for the design and synthesis of novel compounds with significant biological activities [11,12].

The incorporation of pyridine motif into drug molecules have the advantage that it acts as a bioisoster for benzene ring, and such

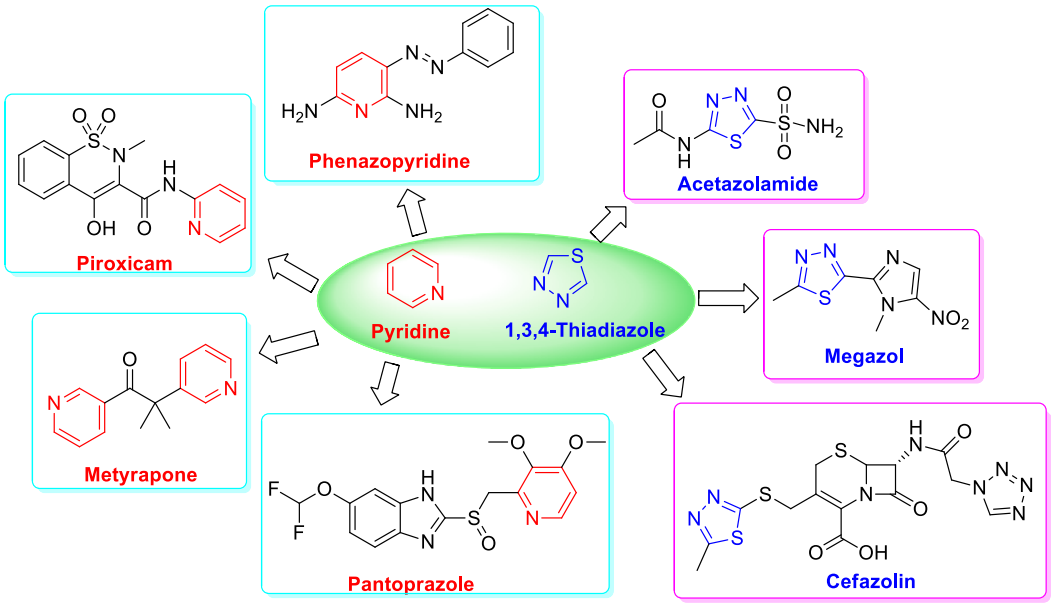

Fig. 1. Structures of pyridine and 1,3,4-thiadiazole containing drug molecules.

isosteric replacement with pyridine may lead to changes in physicochemical properties, such as acidity/basicity and lipophilicity, affecting drug-receptor interactions. Additionally, pyridine is a weak base with a pKa value around 5.2. This makes it more basic than benzene and allows pyridine-containing compounds to interact with acidic functional groups in biological molecules, such as protonated amine functionalities of proteins. The nitrogen atom in the pyridine ring can act as a hydrogen bond acceptor. This property is essential in mediating interactions with biological macromolecules, including enzymes and receptors. Due to its excellent physicochemical and biological profiles pyridine template serves as the essential moiety in many drugs like metyrapone, piroxicam (anti-inflammatory), phenazopyridine (urinary tract analgesic), omeprazole, pantoprazole (antiulcer), Tacrine(anti-alzheimer's), isoniazid (antitubercular), nicorandil (vasodilator), and nikethamide (respiratory stimulant) (Fig. 1) [13–20].

On the other hand, thiadiazole ring existing in four distinct isomeric forms (1,2,3-, 1,2,4-, 1,2,5-, and 1,3,4-thiadiazole), is highly adaptable structural foundations within the field of medicinal chemistry [21]. These isomers demonstrate significant promise as versatile platforms with substantial therapeutic potential. Among the four isomeric forms, 1,3,4-thiadiaozle is one of the best moieties that is commonly synthesized by medicinal chemists in order to develop newer compounds with diverse biological activities [22]. This is due to the fact that 1,3,4-thiadiazole serves as a bioisoster, akin to pyrimidine and oxadiazole. Given the widespread occurrence of pyrimidine in natural compounds, it's not surprising that thiadiazole offer substantial therapeutic promise. The presence of a sulfur atom in thiadiazoles enhances their lipid solubility, while their mesoionic nature facilitates better membrane penetration, the effective passage of derivatives through cellular membranes while establishing strong interactions with biological targets. This attribute enhances the prospect of these compounds having low toxicity and increased selectivity [23–26]. These characteristics attribute for the incorporation of this ring in drugs including carbonic anhydrase inhibitors-acetazolamide, methazolamide; antiprotozoal drug-megazol; antibacterial drugs-cephazolin, cefazedone, sulfamethizole [27–29] (Fig. 1).

Furthermore, several research groups, such as Abd El-Lateef et al. (2023) [30] and Bian et al. (2021) [31], have recently highlighted the efficacy of pyridine derivatives, particularly in demonstrating potent anti-inflammatory properties (Fig. 2). These compounds have also exhibited promising activities in areas like anticancer [32–37]. Notably, Zaher et al. (2022) and Maddila et al. (2016) have contributed significant findings regarding pyridine derivatives' anti-inflammatory [38,39] and anticancer [40–43] effects, respectively, attributed to the presence of the thiadiazole ring within their chemical structures. Moreover, recent developments have seen the integration of pyridine and thiazole rings into lead compounds for anti-inflammatory purposes [44–52]. Fig. 2 depicts the structures of selected potent compounds highlighted in the aforementioned literature.

In view of the above facts, we contemplated that incorporating both pyridine and 1,3,4-thiadiazole nucleus into the same molecule connected through a carbonyl thiourea spacer group would help in the development of new class of anti-inflammatory agents. The basic structural scaffold incorporating two key pharmacophoric pyridin-3-yl and 1,3,4-thiadiazol-2-yl ring systems linked through a unique carbonyl thiourea moiety was designed and the 5th position of 1,3,4-thiadiazol-2-yl system was substituted with various aryl groups to obtain the target molecules. Hence, we designed, synthesized and tested anti-inflammatory activity for a series of novel pyridine linked 1,3,4-thiadiazole derivatives (Fig. 3).

2. Materials and methods

2.1. General

We obtained the necessary chemicals and reagents from S.D. Fine Chemicals to conduct our synthesis. We determined the melting points of the resulting compounds using a Galen Kamp melting point apparatus. FT-IR spectra were acquired using the KBr-Pellet method using a Thermo Nicolet Nexus 670 spectrophotometer. For ^{1}H NMR and ^{13}C NMR spectra, as well as mass spectra, we utilized a Bruker Avance (operating at 300 MHz) and a Polaris Q mass spectrometer, respectively. To monitor the progress of the reactions, we conducted thin-layer chromatography (TLC) on aluminium TLC plates coated with silica gel F_{254} from Merck, Germany. We visualized the spots on the TLC plates using iodine vapours and a UV lamp.

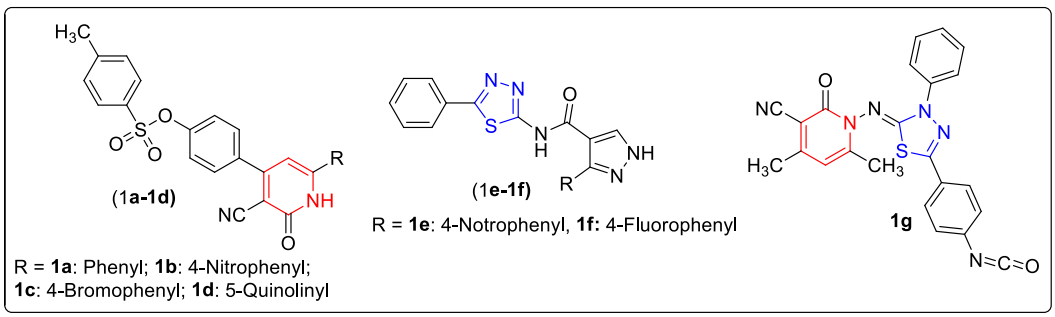

Fig. 2. Structures of selected pyridine and thiadiazole derivatives with potential anti-inflammatory activity.

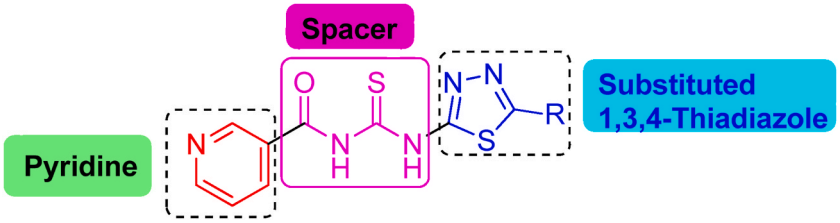

Fig. 3. General structure of the designed compounds.

2.2. Experimental

2.2.1. Synthesis of the nicotinoyl chloride and nicotinoyl isothiocyanate

Nicotinic acid (12.3 g, equivalent to 0.1 mol) was placed into a three-necked flask, which was equipped with a tightly sealed mechanical stirrer, a reflux condenser safeguarded with a calcium chloride tube, and a dropping funnel. The mechanical stirrer was activated, and a gradual stream of 25 mL (40.9 g, corresponding to 6.9 mol) of distilled thionyl chloride was introduced over a span of 15–20 min [53]. Once the addition was finished, the mixture was subjected to heating on a steam bath with continuous stirring for a period of 1 h. Subsequently, the reflux condenser was exchanged for one configured for downward distillation, and any surplus thionyl chloride was eliminated *via* distillation under reduced pressure while maintaining heating on the steam bath. The reaction mixture was then set aside for 24 h to obtain a solid product. The product was further separated and washed with ether to get a colourless solid [54]. After dissolving nicotinoyl chloride (4.24 g, equivalent to 1 mmol) in 150 mL of acetone and agitating it for 1 h, ammonium thiocyanate (2.28 g, 10 mmol) was introduced at room temperature. Once the reaction was deemed complete, as confirmed by TLC monitoring, the reaction mixture was filtered to isolate the precipitated nicotinoyl isothiocyanate (Scheme 1).

2.2.2. Synthesis of 5-substituted-2-amino-1,3,4-thiadiazole derivatives

Thiosemicarbazide (9.11 g, equivalent to 0.1 mol), along with different carboxylic acids (0.1 mol), and concentrated sulfuric acid (5 mL), underwent refluxing for 1.5 h [55]. The reaction's progress was observed using TLC. The resulting mixture was then poured onto crushed ice, followed by filtration. The remaining residue was washed with cold water and subjected to recrystallization in ethanol (Scheme 2).

2.2.3. Synthesis of N-((5-substituted-1,3,4-thiadiazol-2-yl)carbamothioyl)nicotinamide

The equimolar concentration of 5-substituted-2-amino-1,3,4-thiadiazole derivatives (0.1 mol) of step 2and nicotinoylisothiocyanate (0.1 mol) were dissolved in acetone and refluxed [56] to get the target pyridine linked 1,3,4-thiadiazole derivatives (**NTD1-NTD5**) (Scheme 3).

2.2.3.1. N-((5-methyl-1,3,4-thiadiazol-2-yl)carbamothioyl)nicotinamide (NTD1). Brown solid color; R_f = 0.45 (mobile phase: hexane: ethyl acetate, 6:4, v/v visualization: UV and I_2 vapours); %Yield: 84; m.p: 236–238 °C; M.F: $C_{10}H_9N_5OS_2$; MW: 279.02 g/mol; FT-IR (KBr, cm^{-1}): 3451.51 (Ar-C-H str), 2974.21 (Aliphatic-C-H str), 1637.77 (C═C str), 1762.32 (C═N str), 1652.25 (C═O), 1020.20 (C–C str), 851.60 (Ar-CH str); ^{1}H NMR (300 MHz, DMSO) δ ppm: 2.69 (s, 3H, –CH_3), 7.53–9.60 (m, 4H, Pyridine), 11.03 (s, 1H, –NH), 12.10 (s, 1H, –NH); ^{13}C NMR (300 MHz, DMSO) δ ppm: 50.3, 125.0, 128.5, 129.1, 131.1, 132.5, 141.3, 143.1, 164.5, 172.3; MS (*m/z*): [M+1], 280.02.

2.2.3.2. N-((5-phenyl-1,3,4-thiadiazol-2-yl)carbamothioyl)nicotinamide (NTD2). Colourless solid; R_f = 0.63 (mobile phase: hexane: ethyl acetate, 6:4, v/v visualization: UV and I_2 Vapours); %Yield: 79; m.p: 281–283 °C; M.F: $C_{15}H_{11}N_5OS_2$; MW: 341.04 g/mol; FT-IR (KBr, cm^{-1}) 3153.61 (Ar-C-H str), 3089.23 (N–H str), 1724.27 (C═N str), 1718.59 (C═C str), 1635.24 (C═O), 1214.78 (C–C str), 1105.24 (C═S str), 851.60 (Ar-CH str); ^{1}H NMR (300 MHz, DMSO) δ ppm: 7.53–9.10 (m, 4H, Pyridine), 7.64–7.97 (m, 5H, Ar–H),

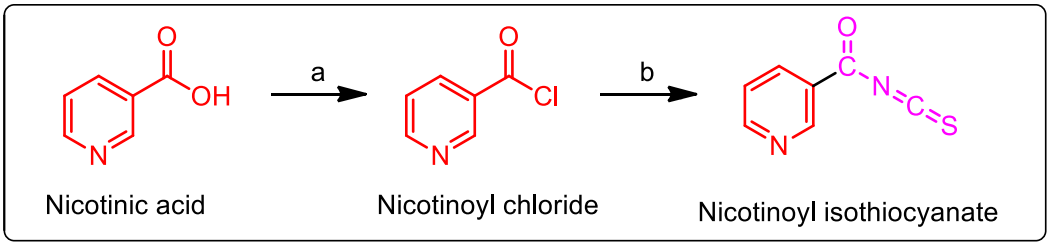

Scheme 1. Synthesis of nicotinoyl chloride and nicotinoyl isothiocyanate a) thionyl chloride ($SOCl_2$), stirring for 15–20 min; b) Ammonium thiocyanate (NH_4SCN), Acetone, Stirring for 1 h, rt.

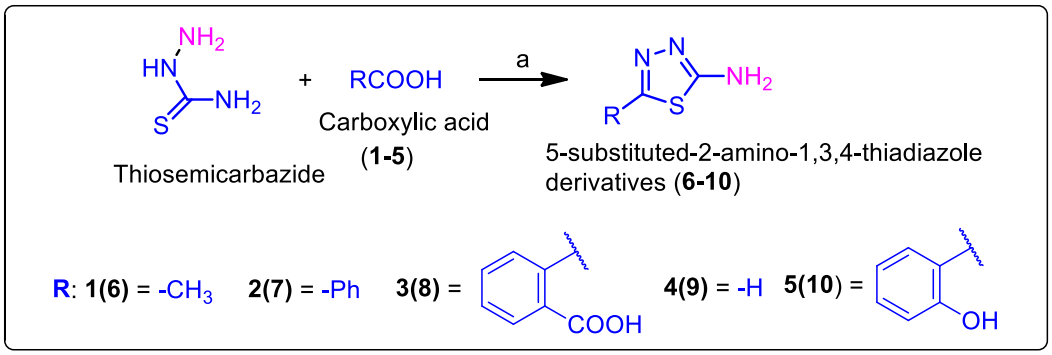

Scheme 2. Synthesis of 5-substituted-2-amino-1,3,4-thiadiazole derivatives a) Ethanol, conc. H_2SO_4, reflux for 1.5 h.

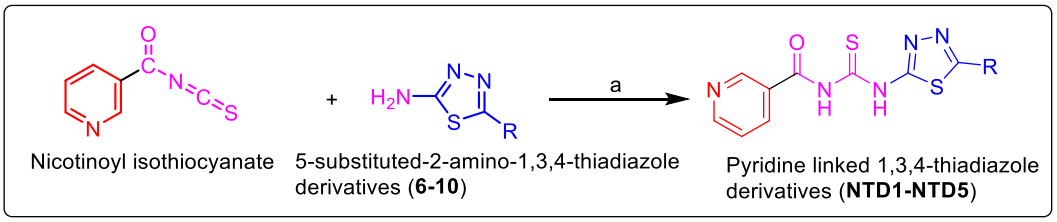

Scheme 3. Synthesis ofpyridine linked 1,3,4-thiadiazole derivatives (**NTD1-NTD5**) a) Reflux in the presence of acetone.

11.46 (s, 1H, –NH), 12.08 (s, 1H, –NH); ^{13}C NMR (300 MHz, DMSO) δ ppm: 125.1, 127.4, 128.3, 128.6, 130.7, 130.8, 134.0, 135.3, 138.4, 141.2, 145.2, 148.7, 163.7, 167.2, 176.4; MS (*m/z*): [M+1], 342.04.

2.2.3.3. 2-(5-(3-nicotinoylthioureido)-1,3,4-thiadiazol-2-yl)benzoic acid (NTD3). Yellow solid; R_f = 0.59 (mobile phase: hexane: ethyl acetate, 6:4, v/v visualization: UV and I_2Vapours), %Yield: 74; m.p: 314–317 °C; M.F: $C_{16}H_{11}N_5O_3S_2$; MW: 385.03 g/mol; FT-IR (KBr, cm^{-1}) 3153.07 (N–H, str), 1747.16 (C═N, str), 1692.24 (C═C, str), 1648.42 (C═O), 1210.23 (C–C, str), 1184.56 (C═S, str); ^{1}H NMR (300 MHz, DMSO) δ ppm: 7.24–7.98 (m, 4H, Ar–H), 7.51–8.95 (m, 4H, Pyridine), 11.15 (s, 1H, –NH), 12.03 (s, 1H, –OH), 12.47 (s, 1H, –NH); ^{13}C NMR (300 MHz, DMSO) δ ppm: 124.1, 126.1, 128.1, 128.4, 129.5, 130.2, 130.9, 131.2, 134.5, 135.1, 148.4, 152.3, 165.4, 169.5, 172.5, 177.8; MS (*m/z*): [M+1], 386.03.

2.2.3.4. N-((1,3,4-thiadiazol-2-yl)carbamothioyl)nicotinamide (NTD4). Brown color solid; R_f = 0.38 (mobile phase: hexane: ethyl acetate, 6:4, v/v visualization: UV and I_2Vapours); %Yield 69; m.p. 320–323 °C; M.F:$C_9H_7N_5OS_2$; MW: 265.01 g/mol; FT-IR (KBr, cm^{-1}) 3154.00 (-NH_2), 1731.56 (C═C str), 1672.00 (C═O str), 1281.27 (C–C str), 1192.20 (C═S str); ^{1}H NMR (300 MHz, DMSO) δ ppm: 7.51–9.60 (m, 4H, Pyridine), 9.23 (s, 1H, C–H), 11.06 (s, 1H, –NH), 12.01 (s, 1H, –NH); ^{13}C NMR (300 MHz, DMSO) δ ppm: 121.0, 124.3, 126.1, 128.4, 130.2, 152.2, 156.5, 177.1, 167.2; MS (*m/z*): [M+1], 266.01.

2.2.3.5. N-((5-(2-hydroxyphenyl)-1,3,4-thiadiazol-2-yl)carbamothioyl)nicotinamide (NTD5). Purple colour solid; R_f = 0.61 (mobile phase: hexane: ethyl acetate, 6:4, v/v visualization: UV and I_2Vapours); %Yield: 81; m.p: 342–346 °C; M.F. $C_{15}H_{11}N_5O_2S_2$; MW: 357.04 g/mol; FT-IR (KBr, cm^{-1}) 3153.68 (-OH), 3097.23 (Ar-CH str), 1768.26 (C═N str), 1761.56 (C═C str), 1662.82 (C═O), 1288.71 (C–C str); ^{1}H NMR (300 MHz, DMSO) δ ppm: 6.24–6.27 (m, 4H, Ar–H), 7.33–7.60 (m, 4H, Pyridine), 10.23 (s, 1H, Ar-OH), 11. 14 (s, 1H, –NH), 12.23 (s, 1H, –NH); ^{13}C NMR (300 MHz, DMSO) δ ppm: 117.2, 121.8, 123.4, 124.1, 127.1, 128.3, 129.4, 130.9, 132.3, 134.2, 141.0, 145.2, 175.2, 168.1, 174.1; MS (*m/z*): [M+1], 358.04.

2.2.4. In vivo studies

The *in vivo* experimental studies including acute oral toxicity and carrageenan–induced rat paw edema model was approved by Institutional Animal Ethical Committee (IAEC) Animal facility, Department of Pharmaceutical Sciences, Vignan's Foundation for Science Technology and Research (Deemed to be University), Vadlamudi, Guntur (Approval Number: VFSTR2046/IEAC/IV/2022-10).

2.2.4.1. Acute oral toxicity. In the current investigation, we evaluated the toxicity of the target compounds (**NTD1-NTD5**) using the acute toxic class method, as outlined by the OECD 423 guidelines. For this study, Swiss albino rats with a body weight ranging from 200 to 250 g were employed. Within each group, three rats of the same gender were included to assess the toxicity of the synthetic derivatives. The initial dosage administered was 200 mg/kg body weight. Prior to treatment, female rats underwent a 3–4 h fasting period during which they were deprived of both food and water. Following the fasting period, the animals' weights were recorded, and

the synthetic derivatives were administered orally at a dose of 200 mg/kg body weight [57]. Subsequently, the animals were meticulously observed at 30-min intervals for the first 4 h after the administration of the test substance, followed by hourly observations for up to 24 h. This monitoring continued daily for a total of 14 days, with each animal being individually scrutinized for any unusual changes in their physical, behavioural, or biological conditions [58].

2.2.4.2. Carrageenan–induced rat paw edema model. In the experiment involving carrageenan-induced paw edema [59], we utilized healthy rats with body weights falling within the range of 100–190 g, regardless of their gender. These rats were divided into three groups, each consisting of six test animals. Prior to the commencement of the experiment, the animals underwent overnight fasting, with access to water provided as needed [60]. In the control group (negative control), a normal saline solution was administered, whereas the second group received **NTD1** at a dosage of 20 mg/kg, the third group received **NTD2,** the fourth group received **NTD3**, and the fifth group was administered the standard drug diclofenac at a dose of 4.5 mg/kg. Each test and standard substance, dissolved in normal saline, was orally administered using an oral catheter [61]. To induce edema, a 0.2 mL solution of 1 % w/v carrageenan was injected into the sub plantar region of the right paw of the rats. The paw was marked with ink at the level of the lateral malleolus, and it was subsequently submerged in mercury up to the marked point. The volume of edema in the rat's paw was then measured using a plethysmometer [62]. The paw volume of each group was assessed right away (at 0 h) and then at 1-h intervals for the subsequent 2 h after carrageenan injection. The actual increase in paw size was calculated by measuring the difference between the initial and final measurements. Rats treated with medications were compared to untreated control rats to determine the average increase in paw size, and a formula was employed to calculate the percentage by which edema development was inhibited [63].Where,

'Vc' represents edema volume in the control.

'Vt' represents edema volume in the group treated with the test drug. The values are mean±SEM (standard error of the mean) of six animals in each group, statistically significant from control, $p<0.001$ % inhibition given in parenthesis. Statistical analysis was performed by ANOVA followed by Tuckey's test.

2.2.5. In silico studies

2.2.5.1. Molecular docking. Molecular Docking and simulation studies were performed using Chemoffice 2016 tools, Discovery Studio 2020 software, AutodocVina module of PyRx 0.8 software [64–66], a DELL workstation running the 64-bit Ubuntu 22.04 LTS operating system, an Intel Core i5-12400 processor clocked at 2.30 GHz, 16 GB of RAM, and an 8 GB Nvidia GeForce RTX 3050 GPU, Desmond module of the Schrodinger Suite, (created by the D.E. Shaw research team and used under an academic license) [67]. The co-crystal protein structure was downloaded from the Protein Data Bank (www.pdb.com or www.rcsb.com) [68]. The target protein cyclooxygenase 2 (COX-2) X-ray crystal structure, co-crystallized with Diclofenac (PDB ID: 1pxx), was downloaded from the protein data bank (www.rcsb.com/www.pdb.com). The protein was prepared by removing water molecules, adding polar hydrogens, removing HET atoms, and checking for missing amino acid residues using the Discovery Studio Visualizer 2021 software, and the file was saved in.pdb format. The target compounds' 2D structures **(NTD1-5)** were drawn in ChemDraw Professional and saved as.pdb files. Using the macromolecule option in the Autodock tool of the PyRx Virtual screening program 0.8, the protein.pdb file was transformed into.pdbqt format. The ligand files were subjected to energy minimization (force field-off) using the Open Babel tool, and conformers (Autodock.pdbqt files) were subsequently generated. The macromolecule (protein pdbt file) and ligands were chosen using Vina Wizard to do the docking technique (auto dock.pdbqt files). By drawing a grid box around the area where the co-crystal ligand exhibits iterations with amino acids, the active binding site of the protein was specified to dock ligands. The ligands with the lowest binding energies were candidate molecules with a high affinity for the target protein. The Discovery Studio Visualizer 2021 program was used to visualize the binding interactions.

2.2.5.2. Molecular dynamics simulation. Molecular dynamics (MD) simulation is a computational method that provides valuable insights into the structural stability and flexibility of protein-ligand complexes (PLCs) and helps understand the thermodynamics of protein-ligand interactions [69]. In this study, MD simulation was performed using the Schrodinger Suite Desmond module to investigate the stability and ligand-binding constancy of the protein-ligand complexes (*COX-2-Internal ligand/diclofenac and COX-2-**NTD3***). To perform MDS, a simulation box was prepared using the orthorhombic geometry and the Simple Point Charge (SPC) explicit water model [70]. Using the cubic SPC water model, the protein-ligand complex was solvated, neutralized with counter ions and physiological salt, and identified using the OPLS AA force field [71]. The system was then energy-minimized using a hybrid algorithm with one thousand steps of steepest, descent, and conjugate gradient algorithms. Using the Reversible Reference System Propagator Algorithms (RESPA) integrator, the system was maintained at a constant temperature of 310.10 K and pressure of 1.0 bar for the duration of the MD simulation (100ns) [72], the Martyna-Tobias-Klein barostat and the Nose-Hoover chain thermostat [73]. The isothermal–isobaric ensemble was used to keep the number of particles, temperature, and pressure constant throughout the simulation [74]. Trajectory files were generated during the simulation, and the *_out.cms* files were downloaded to visualize the trajectories for further analysis. The simulation interaction diagram analysis tab was employed to generate the data for the simulation. The stability of the ligand and protein complex during the simulation was determined by aligning the protein backbone frames with the previous frame, and the interactions of the ligand with active site residues were determined by generating a simulated interaction diagram and selecting the Root Mean Square Deviation (RMSD) using *_out.cms* files.

The thermal_MMGBSA.py script from the Prime/Desmond module of the Schrodinger suite was used to perform the post-simulation MM-GBSA analysis (***Institute license: BIT Mesra***). The MM-GBSA method is a commonly used approach to calculate the free energy of

ligand-protein interactions. The calculation was performed using 200 frames of the 100 ns MD simulation data, and the binding energy was calculated as the MM-GBSA ΔG_{Bind}, which can be calculated by the Prime Energy, an Implicit Solvent Energy Function of Molecular Mechanics, in kcal/mol.

2.2.5.3. Drug likeness analysis. The structures were drawn using the ChemDraw Professional 16 software (ChemDraw® Ultra, version 16, Cambridge Soft Corp., USA), the SMILES of the drawn structures were copied and pasted in the SwissADME server: http://www.swissadme.ch/(accessed on March 3, 2024). The "Run" icon was then pressed to provide the ADMET parameters and associated values.

3. Results and discussion

3.1. Acute oral toxicity study

The acute toxicity assessment serves as a crucial component in evaluating the safety profile of novel chemical entities intended for therapeutic applications. In adherence to the OECD guideline-423 methodology, our study meticulously examined the synthesized pyridine-based thiadiazole derivatives (**NTD1-NTD5**) to ascertain their potential toxicity levels. Utilizing a starting dose of 200 mg/kg body weight administered orally to experimental animals, we observed no discernible evidence of toxicity throughout the 14-day monitoring period following sample administration. Our rigorous observation regimen encompassed a comprehensive assessment of central nervous system (CNS) function, autonomic nervous system (ANS) responses, salivation patterns, skin colouring variations, motor activity, and other general indicators of toxicity. The LD_{50} value, a pivotal indicator of acute toxicity, classifies compounds based on their toxicity levels. Our findings positioned the synthesized compounds within class 5, indicating a notable absence of toxicity at the aforementioned dose level. Notably, this classification underscores the favourable safety profile exhibited by the tested derivatives. Among the synthesized compounds, **NTD4** and **NTD5** exhibited toxic responses, highlighting the importance of discerning variations in chemical structures that may influence toxicity outcomes. Conversely, **NTD1**, **NTD2**, and **NTD3** demonstrated a remarkable lack of toxicity, establishing them as well-tolerated entities with LD50 values exceeding 200 mg/kg body weight. This compelling evidence underscores the promising safety profile of these compounds, bolstering their potential for further development as therapeutic agents. The absence of acute toxicity observed in **NTD1**, **NTD2**, and **NTD3** is particularly encouraging, as it aligns with our overarching goal of identifying novel anti-inflammatory agents with favourable safety profiles. These compounds not only demonstrated significant anti-inflammatory activity, surpassing the efficacy of the standard drug diclofenac, but also exhibited a notable absence of acute toxicity, further underscoring their potential as safe and efficacious therapeutic candidates. In conclusion, our expanded acute toxicity study reinforces the favourable safety profile of the synthesized pyridine-based thiadiazole derivatives, particularly **NTD1**, **NTD2**, and **NTD3**, thereby laying a solid foundation for their continued evaluation and development as prospective anti-inflammatory agents.

3.2. In vivo rat paw edema method

Rat paw edema (Carrageenan-induced) was used to determine the synthetic compounds' anti-inflammatory efficacy. The activity was examined at doses of 20 mg/kg body weight, and the effects were timed at 0 min, 30 min, 1 h, and 2 h. The results are given in Table 1. The anti-inflammatory effects of the three produced substances ranged from slight to strong. For up to 2 h, all three substances showed their peak action. The maximum inhibitory activity was observed when R was substituted with phenyl, methyl, and phenyl carboxylate, according to the data from the synthesized compounds at a dose of 20 mg/kg body weight [75].

The anti-inflammatory activity of synthesized derivatives (**NTD1-NTD3**) compared with the standard drug diclofenac is represented in Fig. 4 and the data suggests that these the three compounds have remarkable ($p < 0.05$) anti-inflammatory activity. The high significant action was seen for the synthesized compounds at 60 and 120 min with significant $p < 0.01$, and $p < 0.001$) activity. This study demonstrates how the target compounds blocked prostaglandins, particularly during the biphasic response following carrageenan administration. In addition, these derivatives have the potential to selectively inhibit the cyclooxygenase enzyme. In Fig. 5 it is clearly demonstrated the difference in test animals with paw edema before and after treatment with the tested synthetic compounds.

Table 1
Effect of selected derivatives on paw edema in rats.

S. No.	Name	Paw edema volume (mm)			
		0 min	30 min	60 min	120 min
1	Control	0.33 ± 0.04	0.33 ± 0.04	0.23 ± 0.02	0.31 ± 0.01
2	Diclofenac (4.5 mg/kg)	0.51 ± 0.01	0.41 ± 0.01*	0.30 ± 0.00**	0.21 ± 0.00***
3	**NTD1** (20 mg/kg)	0.56 ± 0.03	0.43 ± 0.02	0.41 ± 0.01*	0.21 ± 0.01***
4	**NTD2** (20 mg/kg)	0.82 ± 0.08	0.71 ± 0.04	0.40 ± 0.02*	0.31 ± 0.01*
5	**NTD3** (20 mg/kg)	0.50 ± 0.02	0.41 ± 0.01*	0.35 ± 0.02**	0.31 ± 0.01*

n = 6, values are expressed in mean ± SEM, *$p < 0.05$, **$p < 0.01$, ***$p < 0.001$ Assessed using two-way ANOVA followed by Tukey's multiple comparison test.

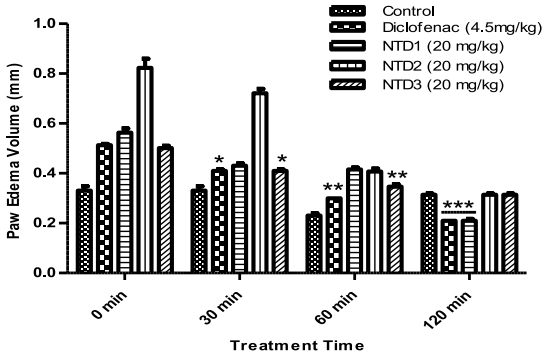

Fig. 4. Effect of selected derivatives on paw edema in rats: *p < 0.05, **p < 0.01, ***p < 0.001 Assessed using two-way ANOVA followed by Tukey's multiple comparison test.

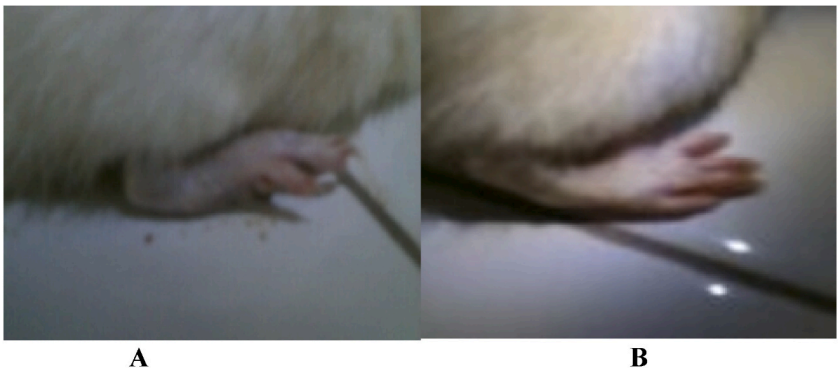

Fig. 5. Anti-inflammatory activity in Wistar rats. A: Paw edema before treatment; B: Paw edema after treatment.

3.3. *In silico studies*

3.3.1. *Molecular docking studies*

The cyclooxygenase 2 (COX-2) protein was selected for *in silico* anti-inflammatory activity screening as the target because this protein plays the major role in the formation of inflammatory mediators like prostaglandins [76]. The docking study results of the title derivatives against the selected protein (PDB ID: 1pxx) are given in Table 2. The results revealed that the derivatives **NTD2,** and **NTD3** showed strong binding affinities with least binding energies −8.5, and −8.4 kcal/mol respectively when compared to co-crystal ligand diclofenac having binding energy −8.4 kcal/mol. The binding energies of all the compounds are given in Table 2. However, the derivativespossess aryl (**NTD2** having benzene**)** substitution or substituted aryl **(NTD3** having benzoic acid**)** substitution on the thiadiazole ring and show significant binding affinities by interacting with amino acid residues in the active site of target protein compared to the internal ligand through different hydrogen and hydrophobic interactions given in Table 3 and depicted in Fig. 6.

The *in silico* results seem merely correlated with the *in vivo* rat paw edema test results which conforms to the validation of *in silico* docking results. Moreover, the research findings reported by Redzicka et al. [77] Soni et al. [78] and Ravichandran et al. [79] reported that compounds with aryl or heteroaryl substitutions may have shown potent anti-inflammatory activity.

3.3.2. *Molecular dynamics simulation analysis*

MD simulation studies were carried out for the Diclofenac-COX-2 (***complex a***) and **NTD3**-COX2 complex (***complex b)***. Root mean

Table 2
Binding energies of the title derivatives against COX-2.

S. No.	Compound	Binding Energy (kcal/mol)
1	**NTD1**	−6.8
2	**NTD2**	−8.5
3	**NTD3**	−8.4
6	**Diclofenac**	−8.4

Table 3
Interactions of the selected derivatives with COX-2 protein active pocket residues.

S. No	Compound	Binding Energy (kcal/mol)	The type of interaction	No. of bonds	Interacting amino acid residues	Bond length (Å)
1	**NTD2**	**−8.5**	H-bond	1	Phe518-S of CH_5N_3S,	2.33
			Hydrophobic	7	Val116, Val349, Leu359, Ala527, Val523, Leu531	3.47 to 5.02
2	**NTD3**	**−8.4**	H-bond	2	Arg120 and Tyr355	2.58 & 2.98
			Hydrophobic	7	Val349, Leu352, Trp387, Met522, Val523, Gly526, Ala527	4.35 to 5.49
3	**Diclofenac**	**−8.4**	H-bond	1	Ser530	2.38
			Hydrophobic	5	Val349, Trp387, Met522, Val523 and Ala527	4.38 to 5.47

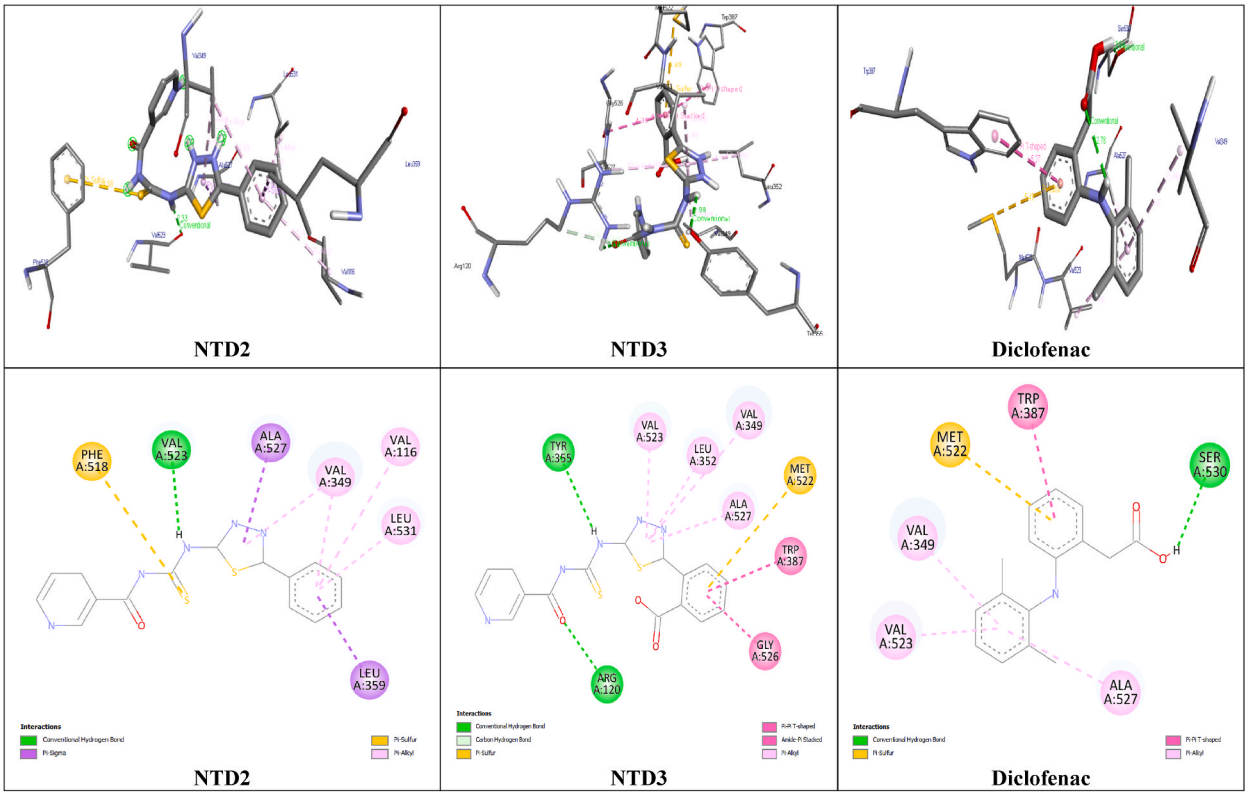

Fig. 6. Interactions of selected derivatives (NTD2 and NTD3) with active pocket residues of COX-2.

square deviation (RMDS) was used to evaluate how well the ligand stays bound to the active site of the chosen target.

RMSD analysis: RMSD analysis of the ligand-protein complex reveals whether equilibrium has been achieved. The RMSD of the protein in the presence of ligand should converge at a constant value of 1–5 Å However, for small biomolecules, minor fluctuations in this range are perfectly acceptable. Moreover, if the protein/ligand undergoes a large conformation change, there might be deviations in RMSD values, but they should converge at a constant value for a particular simulation. Here for ***complex a***; the conformation revealed significant RMSD values in the range 2.5 Å 4.2 Å which displays the stability of the Protein (backbone and c-alpha). Similarly, for ***complex b,*** the RMSD values were in the 2.5–3.5 Å range. However, there were fluctuations in both complexes, but these minor deviations are acceptable. This observation indicates that the protein, in the presence of an external ligand, maintained its conformation without significant changes. Consequently, it effectively accommodated the ligand within the active site. The Ligand RMSD metric is a measure for assessing the stability of the ligand within the protein and its binding pocket. In the simulation of ***complex a***, the RMSD values initially ranged from 1.2 to 1.2 Å (0–50ns). Following this, there were minor fluctuations, after which the RMSD converged to a constant value of 2–3 Å (50–100ns). For ***complex b***, the ligand was stable throughout the simulation with an RMSD value of 2–2.5 Å (0–100ns). There were minor fluctuations with a slight deviation in the RMSD from 55 to 60ns. Therefore, our ligand (**NTD3**) has demonstrated effectiveness in binding to the active site and interacting with the key amino acid residues. Overall, protein-ligand ***complex b*** was found to be more stable than ***complex a*** though in both cases confirmations were maintained constantly throughout the simulation time.

The dynamicity attribute offers a valid criterion to assess the effectiveness of a suggested inhibitor because potentially effective inhibitors should be able to bind firmly to the enzyme and form stable non-dynamic complexes. These findings are consistent with the image presented in Fig. 7a and b, in which the RMSD values can be visually observed.

RMSF stands for root mean square fluctuation and is used in molecular simulations to assess the flexibility and dynamics of atoms or residues within a biomolecular system. It quantifies the average deviation or fluctuation of the positions of atoms or residues from their mean positions throughout the simulation. The RMSF values are typically represented as a plot or graph to visualize the regions of the molecule that experience significant fluctuations during the simulation. A higher RMSF value indicates greater flexibility or movement, whereas a lower RMSF value suggests relative stability or restricted motion. This diagram (Fig. 8a and b) displays the regions of the protein that experience the most significant fluctuations while simulation. The protein tails (C- and N-terminal), which fluctuate more than other sections of the protein, typically correlate to the peaks in the figure. Beta strands and alpha helices, which are secondary structural components, are often more rigid than the protein 's unstructured areas and fluctuate less than loop regions. During the simulation, there were slight size variations in each protein–ligand complex. Green vertical bars indicate ligand interactions and are used to identify the protein residues that interact with the ligand.

Throughout the simulation, ligand and protein interaction were monitored and analyzed. These interactions are classified into different types, which are summarized and depicted in the plot (Fig. 9a and b). There are four basic categories used to classify protein-ligand interactions: hydrogen bonds, hydrophobic interactions, ionic interactions, and water bridges. Protein secondary structures are maintained in large part by hydrogen bonding. These bonds contribute to the stability of protein folding, thereby aiding in the maintenance of alpha helices, beta sheets, and other secondary structural elements. In addition, the presence of hydrogen bond donors and acceptors is a crucial factor in passive diffusion across cell membranes. This process is of utmost importance in the absorption and distribution of drugs within the body, highlighting the significance of hydrogen bonds in pharmacokinetics. According to the graph in Fig. 9, a value of 0.2 indicates that 20 % of the simulation time is spent maintaining the specific interaction. However, values above 1.0 are however feasible as some protein residues may form many interactions with the ligand of the same subtype.

As illustrated in Fig. 9a and **b,** the interactions through hydrogen bonds were found to be maximum during the simulation for **complex b** rather than **complex a**. The number of H-bonds established with the amino acid residues of the proteins was also higher for **complex b** (Arg120: 120 %, Tyr355: 80 %, Tyr385: 50 %, and Ser530: 90 %) than **complex a** (Tyr385: 80 %, and Ser530: 150 %). Compared with the internal ligand, **NTD3** showed increased hydrophobic contacts, ionic interactions, and water-mediated couplings. These results imply that the system's backbone variations were small and that the protein-ligand complex was stable throughout the simulation.

Protein-ligand contacts are an essential aspect of simulating molecular interactions between proteins and ligands because they represent their mode of interaction with each other. The possible interactions (H-bonds, Ionics, Hydrophobic, and Water bridges) with respect to the time were summarized in Fig. 10. The top panel summarizes the total number of distinct interactions made throughout the trajectory between the protein and the ligand. Each trajectory frame in the bottom panel identifies the residues that interact with the ligand. According to the color scale on the right side of the plot, residues that make many specific interactions with the ligand are shown in a darker shade of orange. **NTD3** made more contact with the protein in this instance than it did with the internal ligand. This indicates that **complex b** is more stable than **complex a**.

Detailed ligand interaction analysis in molecular dynamics simulations provides essential information for understanding binding mechanisms, guiding rational drug design, predicting binding free energies, and gaining mechanistic insights into ligand-target interactions. The chosen trajectory (from 0.00 to 100.00 ns) and the interactions that lasted for more than 30.0 % of the simulation period have been highlighted in this article. It is important to note that interactions above 100 % are conceivable because some residues may have several interactions of the same kind with the same ligand atom, resulting in cumulative interaction times that go beyond the simulation's time limit. There were more interactions observed in the case of internal ligand (b) **NTD3** than internal ligand (a) as seen in Fig. 11.

Several ligand properties are of utmost importance in the context of drug design and molecular interactions, these characteristics include the ligand RMSD, rGyr (radius of gyration), molSA (molecular surface area), SASA (solvent accessible surface area), and PSA (polar surface area). A glimpse of these properties is displayed in Fig. 12.

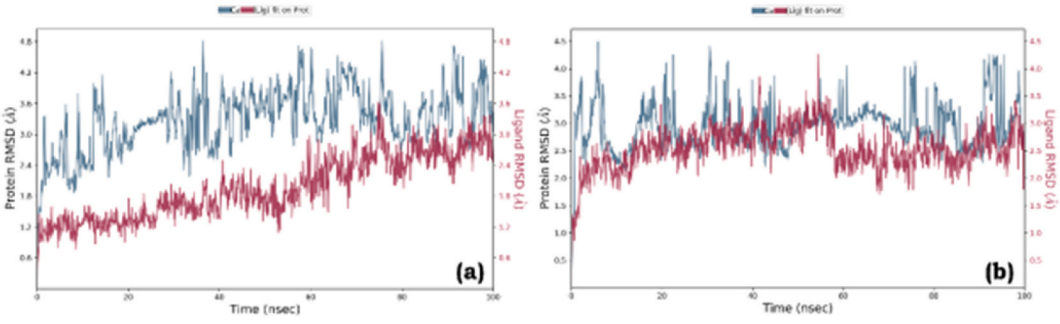

Fig. 7. Root mean square deviation (RMSD) graph of (a) COX-2 protein and co-crystal ligand (Diclofenac) (b) COX-2 protein and **NTD3**.

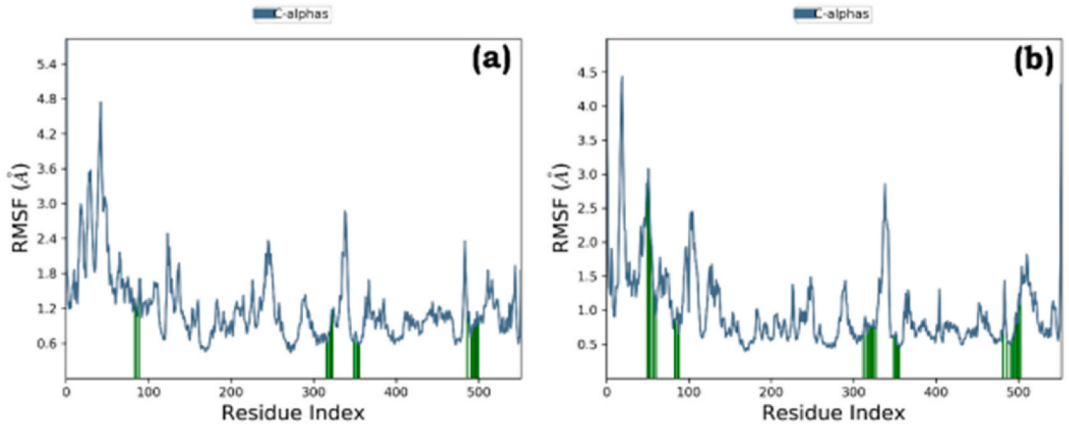

Fig. 8. Root mean square fluctuation (RMSF) graph of (a) COX-2 protein and co-crystal ligand diclofenac, and (b) COX-2 protein and **NTD3**.

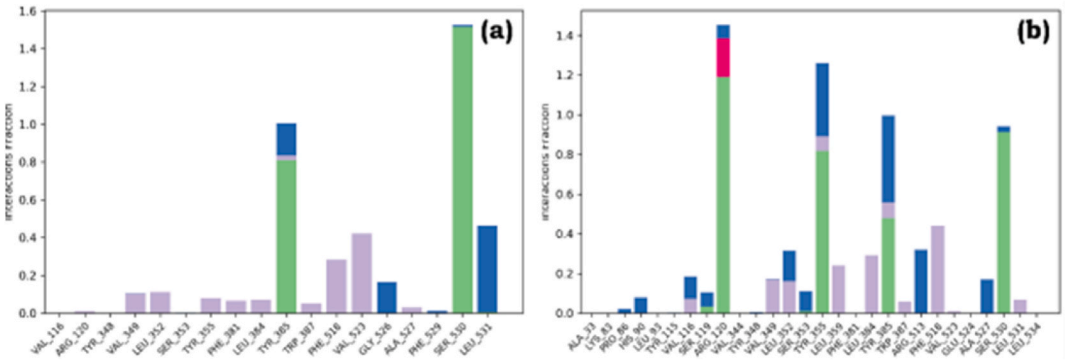

Fig. 9. Plot (stacked bar charts) of ligand-protein interactions during MD simulation of (a) protein-internal ligand (diclofenac) complex and (b) protein-**NTD3** ligand complex. [green: H-bonds, lavender: hydrophobic, pink: ionic, and blue: water bridges]. (For interpretation of the references to color in this figure legend, the reader is referred to the Web version of this article.)

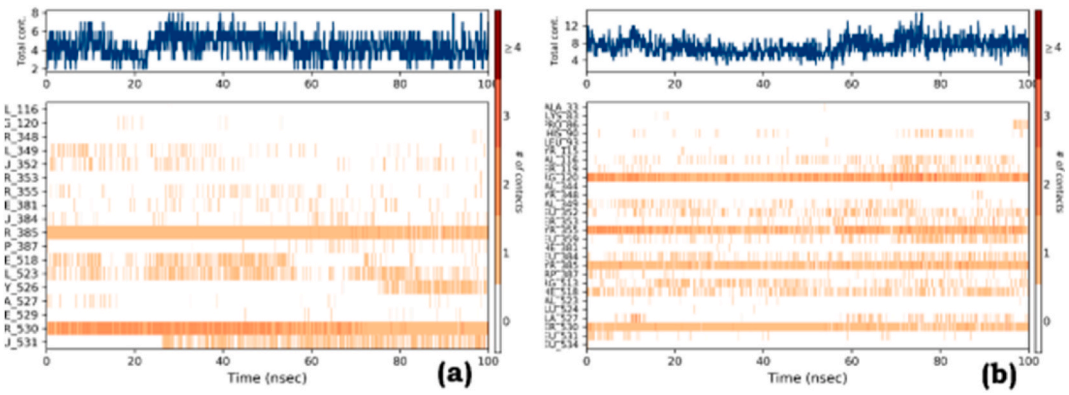

Fig. 10. Specific interactions of the protein with the (a) internal ligand: diclofenac, and (b) **NTD3** throughout the trajectory. (Dark color indicates a more specific contact with the ligand). (For interpretation of the references to color in this figure legend, the reader is referred to the Web version of this article.)

3.3.3. Post-MM-GBSA analysis

The calculated free energy available for binding ΔG average of the (a) internal ligand and (b) **NTD3** was found to be -70.30 ± 6.85 kcal/mol and -68.20 ± 6.25 kcal/mol for PDB ID: IPXX (COX-2 protein).

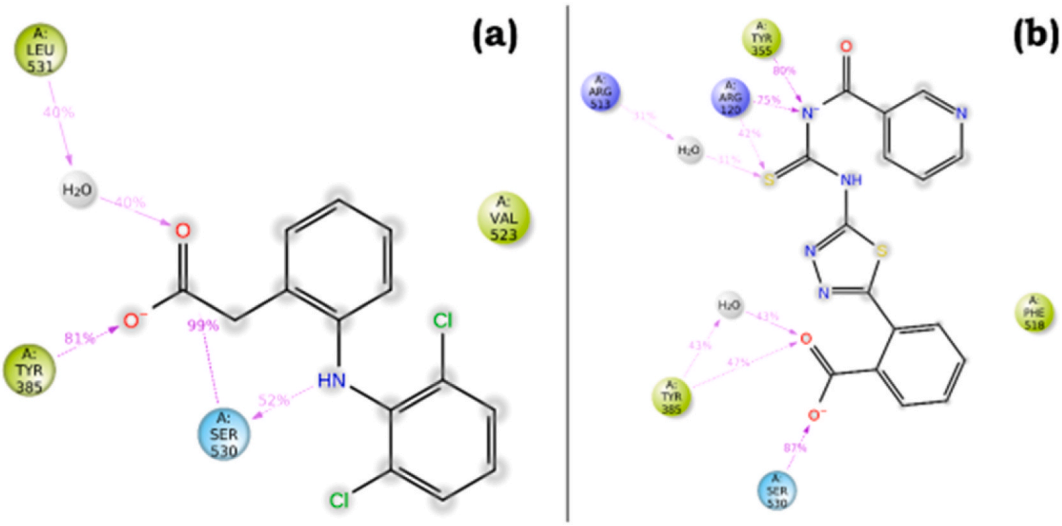

Fig. 11. 2D interactions of amino acid residues of protein with (a) internal ligand: diclofenac, and (b) **NTD3**.

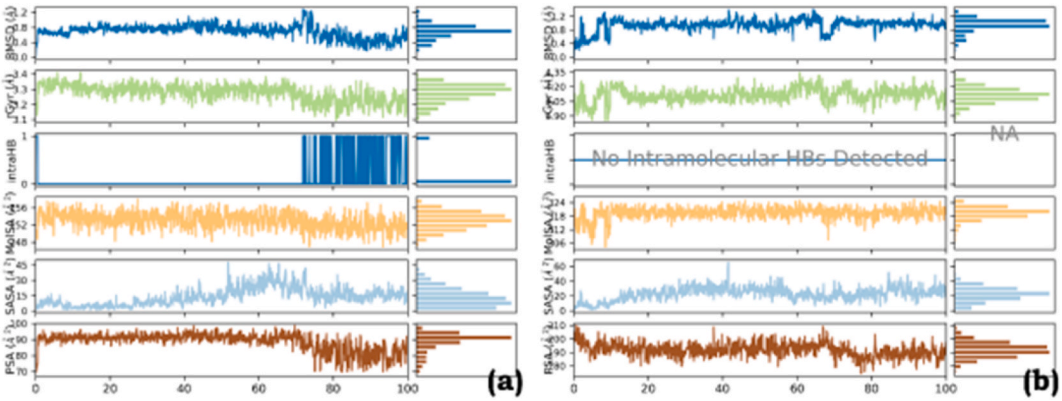

Fig. 12. Representation of the ligand properties of (a) internal ligand: diclofenac, and (b) **NTD3**.

3.3.4. Drug likeness analysis

Drug likeness is defined as the degree of similarity between certain compounds and well-known medications, as demonstrated by a complicated balance of molecular features and structural attributes [80]. Properties of molecules such as hydrophobicity, electronic distribution, hydrogen bonding, molecule weight, pharmacophore entity, bioavailability, reactivity, toxicity, and metabolic stability influence how similar a medicine should be. One of the most popular methods for estimating a compound's permeability and solubility and, thus, predicting whether or not it qualifies as a medication candidate is Lipinski's rule. According to the rule, if a chemical violates the Lipinski rule of five, it is more likely to have poor absorption or penetration if it includes more than five H-bond donors (the sum of NH and OH), more than 500 molecular weight (MWt), more than five log P values, and more than ten H-bond acceptors (the sum of N and O). SwissADME tool is routinely employed by the medicinal chemists in order to assess the drug-likeness and physico-chemical properties required for new lead compounds [81,82]. The drug likeness properties of **NTD3** are given in Table 4 predicted through online tool SwissADME: http://www.swissadme.ch/. Most of the drug likeness properties of **NTD3** were found to be with in the acceptable range which indicated that the proposed potent derivative **NTD3** might have drug likeness properties.

Fig. 13 represent SARs of pyridine-1,3,4-thiadiazole derivatives as anti-inflammatory agents. Compound with phenyl carboxylate substituent (R, C_5) demonstrated increased inhibitory activity, whereas the compound with only phenyl substituent exhibited moderate level of inhibitory activity. The rest of the compounds with or without substituents (methyl, 2-hydroxyphenyl) showed moderate-to-low activity. In molecular docking study, the compound possessing the highest inhibitory activity displayed better ligand-protein molecular interactions including hydrogen bonding and hydrophobic interactions. Other compounds produced considerably less interactions as compared to the best inhibitor. The heteroaryl ring systems of pyridine-1,3,4-thiadiazole scaffold significantly contributed to the hydrophobic interactions, while the linking carbonyl thiourea group participated in polar hydrogen bonding interactions.

Table 4
Drug likeness analysis results of selected NTD3 and Diclofenac.

Compound	Molecular Weight (g/mol)	H-Bond Acceptor	H-Bond Donors	Consensus Log Po/w	Molar Refractivity	GI Absorption	BBB Permeant	Lipenski	Bioavailability Score	PAINS
NTD3	385.42	6	3	2.13	99.71	Low	No	Yes; 0 violation	0.11	0
Diclofenac	296.15	2	2	3.66	77.55	High	Yes	Yes; 0 violation	0.85	0

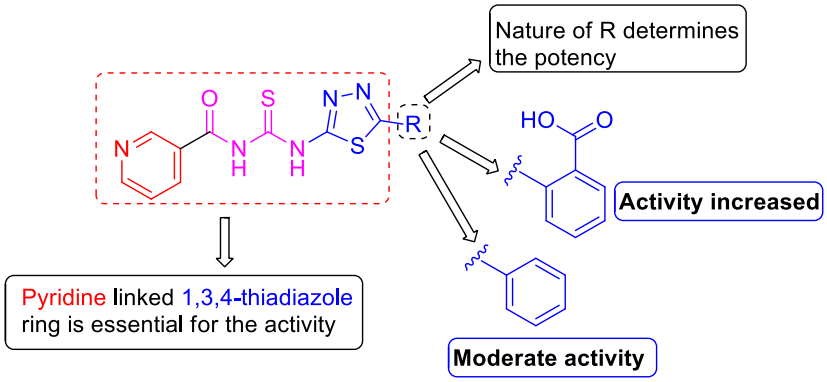

Fig. 13. Structure activity relationship features of pyridine-1,3,4-thiadiazole derivatives.

4. Conclusion

In this comprehensive study, we have meticulously synthesized and characterized a series of novel pyridine-linked 1,3,4-thiadiazole derivatives, denoted as **NTD1-5**, employing a meticulously crafted synthetic procedure. These derivatives underwent a rigorous evaluation encompassing both experimental and computational methodologies to ascertain their potential as anti-inflammatory agents. Our endeavour was not only to identify promising lead compounds but also to shed light on the intricate mechanisms underlying their pharmacological activities. Among the synthesized compounds, **NTD3**, distinguished by its incorporation of benzoic acid, emerged as a standout candidate, demonstrating remarkable anti-inflammatory properties across a spectrum of evaluations. Through meticulous *in vivo* and *in silico* studies, **NTD3** showcased unprecedented efficacy, surpassing even the established anti-inflammatory benchmark, Diclofenac. Its superior binding affinity, stability, and interactions with the COX-2 target protein underscore its potential as a lead compound for future drug development efforts. Crucially, our investigation extended beyond efficacy to encompass safety considerations. Here, we observed that **NTD1, NTD2,** and **NTD3** exhibited a favourable safety profile, evincing no toxicity concerns at tested dosage levels. Conversely, **NTD4** and **NTD5** exhibited undesirable toxic effects, emphasizing the imperative of thorough safety assessments in drug development. The implications of our findings extend far beyond the confines of this study. They offer valuable insights into the intricate interplay between molecular structure and pharmacological activity, paving the way for the development of more efficacious and safer anti-inflammatory therapies. However, while **NTD3** shows promise as a lead compound, further exploration of its structure-activity relationship and mechanistic underpinnings is warranted. Moreover, the drug likeness study results of the **NTD3** indicated that most of the drug likeness proving properties are within acceptable limits and there is no violation in Lipinski rule and PAINS. All these results indicate that the derivative **NTD3** might be a potent anti-inflammatory and be a drug like candidate. In essence, our study represents a significant milestone in the field of drug development, providing a robust foundation for future endeavors. It underscores the potential of **NTD3** as a pivotal candidate in the quest for more effective anti-inflammatory treatments and underscores the importance of integrating multidisciplinary approaches to drug discovery and development. However, further extensive studies are required to elucidate the structural activity studies and lead likeness properties of the potential derivative **NTD3**.

Data availability statement

The complete data related to the work is included in the manuscript itself.

CRediT authorship contribution statement

Naresh Podila: Formal analysis, Data curation, Conceptualization. **Naveen Kumar Penddinti:** Project administration, Formal analysis, Data curation. **Mithun Rudrapal:** Visualization, Validation, Supervision. **Gourav Rakshit:** Visualization, Validation, Resources, Data curation. **Sathish Kumar Konidala:** Writing – original draft, Visualization, Supervision. **Veera Shakar Pulusu:** Data curation, Formal analysis, Visualization. **Richie R. Bhandare:** Funding acquisition, Writing – review & editing. **Afzal B. Shaik:** Writing – review & editing, Writing – original draft, Validation, Software.

Declaration of competing interest

The authors declare that they have no known competing financial interests or personal relationships that could have appeared to influence the work reported in this paper.

Acknowledgement

The authors are thankful to the Management of Vignan's Foundation for Science Technology and Research (Deemed to be University), Guntur and Vikas College of Pharmaceutical Sciences for arranging the necessary facilities and infrastructure to carry out this research work. The author ABS would like to acknowledge St Mary's College of Pharmacy and St Mary's Group of Institutions, Guntur, Andhra Pradesh, India. RRB, UAE would like to thank Deanship of Graduate Studies and Research, Ajman University, UAE for their support in providing assistance in article processing charges of this manuscript.

References

[1] V. Jogpal, M. Sanduja, R. Dutt, V. Garg, Tinku. Advancement of Nanomedicines in chronic inflammatory disorders, Inflammopharmacology 30 (2) (2022) 355–368, https://doi.org/10.1007/s10787-022-00927-x.
[2] S.R. Feldman, L.S. Cox, L.C. Strowd, R.A. Gerber, S. Faulkner, D. Sierka, T.W. Smith, J.C. Cappelleri, M.E. Levenberg, The challenge of managing atopic dermatitis in the United States, American Health Drug Benefits 12 (2) (2019) 83–93.
[3] C. Cadet, E. Maheu, Non-steroidal anti-inflammatory drugs in the pharmacological management of osteoarthritis in the very old: prescribe or proscribe? Therapeutic Advances in Musculoskeletal Disease 13 (2021) 1759720X2110221 https://doi.org/10.1177/1759720x211022149.
[4] S. Drożdżal, K. Lechowicz, B. Szostak, J. Rosik, K. Kotfis, A. Machoy-Mokrzyńska, M. Białecka, K. Ciechanowski, B. Gawrońska-Szklarz, Kidney damage from nonsteroidal anti-inflammatory drugs—myth or truth? Review of selected literature, Pharmacology Research & Perspectives 9 (4) (2021) e00817, https://doi.org/10.1002/prp2.817.
[5] M. Oray, K. Abu Samra, N. Ebrahimiadib, H. Meese, C.S. Foster, Long-term side effects of glucocorticoids, Expet Opin. Drug Saf. 15 (4) (2016) 457–465, https://doi.org/10.1517/14740338.2016.1140743.
[6] W. Zhang, Y. Bai, Y. Wang, W. Xiao, Polypharmacology in drug discovery: a review from systems Pharmacology perspective, Curr. Pharmaceut. Des. 22 (21) (2016) 3171–3181, https://doi.org/10.2174/1381612822666160224142812.
[7] K. Kaur, V. Kumar, G.K. Gupta, Trifluoromethylpyrazoles as anti-inflammatory and antibacterial agents: a review, J. Fluor. Chem. 178 (2015) 306–326, https://doi.org/10.1016/j.jfluchem.2015.08.015.
[8] N. Chandna, S. Kumar, P. Kaushik, D. Kaushik, S.K. Roy, G.K. Gupta, M.J. Sanjay, K.K. Jitander, P.K. Sharma, Synthesis of novel celecoxib analogues by bioisosteric replacement of sulfonamide as potent anti-inflammatory agents and cyclooxygenase inhibitors, Bioorg. Med. Chem. 21 (15) (2013) 4581–4590, https://doi.org/10.1016/j.bmc.2013.05.029.
[9] S. Sharma, D. Kumar, G. Singh, V. Monga, B. Kumar, Recent advancements in the development of heterocyclic anti-inflammatory agents, Eur. J. Med. Chem. 200 (2020) 112438, https://doi.org/10.1016/j.ejmech.2020.112438.
[10] S. Sondhi, M. Dinodia, J. Singh, R. Rani, Heterocyclic compounds as anti-inflammatory agents, Curr. Bioact. Compd. 3 (2) (2007) 91–108, https://doi.org/10.2174/157340707780809554.
[11] U.A. Atmaram, S.M. Roopan, Biological activity of Oxadiazole and thiadiazole derivatives, Appl. Microbiol. Biotechnol. 106 (9–10) (2022) 3489–3505, https://doi.org/10.1007/s00253-022-11969-0.
[12] R.A. Tejeswara, K.K. Naresh, Synthesis of Pyridine Derivatives for Diverse Biological Activity Profiles: A Review, Elsevier eBooks, 2023, pp. 605–625, https://doi.org/10.1016/b978-0-323-91221-1.00005-1.
[13] M.M. Hammouda, M.E. Khaled, M.R. Marwa, M.A.O. Amany, Synthesis and biological activities of Bicyclic pyridines integrated Steroid hybrid, Steroids (2023) 109287, https://doi.org/10.1016/j.steroids.2023.109287.
[14] A.B. Kasetti, S. Indrajeet, R. Nagasuri, B.S. Afzal, Antimicrobial and antitubercular evaluation of some new 5-Amino-1,3,4-thiadiazole-2-thiol derived Schiff bases, Rev. Roum. Chem. 65 (9) (2020) 771–776, https://doi.org/10.33224/rrch.2020.65.9.01.
[15] S.S. Arun, B.S. Afzal, R.M. Jyotshana, R. Synthesis Rajesh, Characterization and biological evaluation of some new 2-Amino-5-Aryl-1,3,4-thiadiazoles as antimicrobial and antitubercular agents, Pharmanest 6 (2) (2015) 2765–2770.
[16] O.O. Ferreira, N.M. Suraj, J. Bhagwat, C. Samir, K. Aleksey, R.B. Richie, B.S. Afzal, Synthesis, *in-silico, In vitro* and DFT assessments of substituted Imidazopyridine derivatives as potential Antimalarials targeting Hemoglobin Degradation pathway, Journal of Computational Biophysics and Chemistry 2 (7) (2023) 795–814, https://doi.org/10.1142/S2737416523500412.
[17] Xiang Zuo, M. Na, Fan Zhijin, Z. Qingxiang, Z. Haike, W. Huan, Zhikun Yang, Synthesis of 4-methyl-1, 2, 3-thiadiazole derivatives *via* Ugi reaction and their biological activities, J. Agric. Food Chem. 58 (5) (2010) 2755–2762, https://doi.org/10.1021/jf902863z.
[18] S. Babu Lagu, P. Yejella Rajendra, Deepthi Doddigopu, B. Shaik Afzal, B. Jagadish, G. Harish, Synthesis and characterization some of cyanopyridine, cyanopyrans from 4′-Triflurometh yacetophenyl, 4′-Triflurometh oxyacetophenyl derivative and their antimicrobial activity, in: Proceedings of International Conference on Drug Discovery (ICDD), 2020. Available at: SSRN:https://ssrn.com/abstract=3528178.
[19] Y. Ling, Z.-Y. Hao, D. Liang, C.-L. Zhang, Y.-F. Liu, Y. Wang, The expanding role of pyridine and Dihydropyridine scaffolds in drug design. Drug design, Development and Therapy 15 (2021) 4289–4338, https://doi.org/10.2147/dddt.s329547.
[20] F.-A. Khan, S. Yaqoob, S. Ali, N. Tanveer, Y. Wang, S. Ashraf, K.A. Hasan, S.A.M. Khalifa, Q. Shou, Z. Ul-Haq, Z.H. Jiang, H.R. El-Seedi, Designing functionally substituted pyridine-Carbohydrazides for potent antibacterial and Devouring Antifungal effect on Multidrug Resistant (MDR) Strains, Molecules 28 (1) (2023) 212, https://doi.org/10.3390/molecules28010212.
[21] B. Sharma, A. Verma, S. Prajapati, U.K. Sharma, Synthetic methods, chemistry, and the Anticonvulsant activity of thiadiazoles, International Journal of Medicinal Chemistry 2013 (2013) 1–16, https://doi.org/10.1155/2013/348948.
[22] T. Anthwal, S. Paliwal, S. Nain, Diverse biological activities of 1,3,4-thiadiazole scaffold, Chemistry 4 (4) (2022) 1654–1671, https://doi.org/10.3390/chemistry4040107.
[23] V.A. Obakachi, Babita Kushwaha, Narva Deshwar Kushwaha, Sithabile Mokoena, AbMajeed Ganai, Tabasum Khan Pathan, Werner, Rajshekhar Karpoormath, Synthetic and anti-cancer activity aspects of 1, 3, 4-thiadiazole containing bioactive molecules: a Concise review, J. Sulfur Chem. 42 (6) (2021) 670–691, https://doi.org/10.1080/17415993.2021.1963441.
[24] Y. Li, J. Geng, Y. Liu, S. Yu, G. Zhao, Thiadiazole-a promising structure in medicinal chemistry, ChemMedChem 8 (1) (2012) 27–41, https://doi.org/10.1002/cmdc.201200355.
[25] Y. Hu, C.-Y. Li, X.-M. Wang, Y.-H. Yang, H.L. Zhu, 1,3,4-Thiadiazole: synthesis, reactions, and applications in medicinal, Agricultural, and materials chemistry, Chem. Rev. 114 (10) (2014) 5572–5610, https://doi.org/10.1021/cr400131u.
[26] M. Szeliga, Thiadiazole derivatives as anticancer agents, Pharmacol. Rep. 72 (5) (2020) 1079–1100, https://doi.org/10.1007/s43440-020-00154-7.
[27] A. Aliabadi, 1,3,4-Thiadiazole based anticancer agents, Anti Cancer Agents Med. Chem. 16 (10) (2016) 1301–1314, https://doi.org/10.2174/1871520616666160628100936.
[28] J. Matysiak, Biological and pharmacological activities of 1,3,4-thiadiazole based compounds, Mini-Rev. Med. Chem. 15 (9) (2015) 762–775, https://doi.org/10.2174/1389557515666150519104057.
[29] X. Han, Long Yu Yun, Y. Hu, Xin Hua Liu, 1,3,4-Thiadiazole: a Privileged scaffold for drug design and development, Curr. Top. Med. Chem. 21 (28) (2021) 2546–2573, https://doi.org/10.2174/1568026621666211111154342.
[30] H.M. Abd El-Lateef, A.A. Abdelhamid, M.M. Khalaf, M. Gouda, N.A. Elkanzi, H. El-Shamy, A.M. Ali, Green synthesis of novel pyridines via one-pot Multicomponent reaction and their anti-inflammatory evaluation, ACS Omega 8 (12) (2023) 11326–11334, https://doi.org/10.1021/acsomega.3c00066.

[31] M. Bian, Q.Q. Ma, Y. Wu, H.H. Du, G. Guo-Hua, Small molecule compounds with good anti-inflammatory activity reported in the literature from 01/2009 to 05/2021: a review, J. Enzym. Inhib. Med. Chem. 36 (1) (2021) 2139–2159, https://doi.org/10.1080/14756366.2021.1984903.

[32] I. Abbas, S. Gomha, M. Elaasser, M. Bauomi, Synthesis and biological evaluation of new pyridines containing imidazole moiety as antimicrobial and anticancer agents, Turk. J. Chem. 39 (2) (2015) 334–346, https://doi.org/10.3906/kim-1410-25.

[33] M.G. Badrey, H.M. Abdel-Aziz, S.M. Gomha, M.M. Abdalla, A.S. Mayhoub, Design and synthesis of imidazopyrazolopyridines as novel selective COX-2 inhibitors, Molecules 20 (8) (2015) 15287–15303, https://doi.org/10.3390/molecules200815287.

[34] S.M. Gomha, K.M. Dawood, Synthetic utility of Pyridinium Bromide: synthesis and antimicrobial activity of novel 2, 4, 6-Trisubstituted pyridines having pyrazole moiety, J. Heterocycl. Chem. 54 (3) (2017) 1943–1948, https://doi.org/10.1002/jhet.2790.

[35] S.M. Gomha, Z.A. Muhammad, M.R. Abdel-aziz, H.M. Abdel-aziz, H.M. Gaber, M.M. Elaasser, One-pot synthesis of new thiadiazolyl-pyridines as anticancer and antioxidant agents, J. Heterocycl. Chem. 55 (2) (2018) 530–536, https://doi.org/10.1002/jhet.3088.

[36] F.M. Abdelrazek, S.M. Gomha, M.E. Shaaban, K.A. Rabee, H.N. El-Shemy, A.M. Abdallah, P. Metz, One-pot three-component synthesis and molecular docking of some novel 2-thiazolyl pyridines as potent antimicrobial agents, Mini Rev. Med. Chem. 19 (6) (2019) 527–538, https://doi.org/10.2174/1389557518666181019124104.

[37] H.M. Abdel-Aziz, S.M. Gomha, A.A. El-Sayed, Y.N. Mabkhot, A. Alsayari, A.B. Muhsinah, Facile synthesis and antiproliferative activity of new 3-cyanopyridines, BMC chemistry 13 (2019) 1–10, https://doi.org/10.1186/s13065-019-0652-1.

[38] N.H. Zaher, M.M. El-Sheikh, R.M. El-Hazek, M.G. El-Gazzar, R.M. El-Hazek, Potential effect of novel thiadiazole derivatives against radiation induced inflammation with low cardiovascular risk in rats, Med. Chem. Res. 31 (11) (2022) 1875–1888, https://doi.org/10.1007/s00044-022-02948-1.

[39] S. Maddila, S. Gorle, C. Sampath, P. Lavanya, Synthesis and anti-inflammatory activity of some new 1, 3, 4-thiadiazoles containing pyrazole and pyrrole nucleus, J. Saudi Chem. Soc. 20 (2016) S306–S312, https://doi.org/10.1016/j.jscs.2012.11.007.

[40] S.M. Gomha, T.A. Salaheldin, H.M. Hassaneen, H.M. Abdel-Aziz, M.A. Khedr, Synthesis, characterization and molecular docking of novel bioactive thiazolyl-thiazole derivatives as promising cytotoxic antitumor drug, Molecules 21 (1) (2015) 3, https://doi.org/10.3390/molecules21010003.

[41] S. Gomha, H.M. Abdel-aziz, Synthesis and antitumor activity of 1, 3, 4-thiadiazole derivatives bearing coumarine ring, Heterocycles 91 (3) (2015) 583–592, https://doi.org/10.3987/COM-14-13146.

[42] G.F. Aljohani, T.Z. Abolibda, M. Alhilal, J.Y. Al-Humaidi, S. Alhilal, H.A. Ahmed, S.M. Gomha, Novel thiadiazole-thiazole hybrids: synthesis, molecular docking, and cytotoxicity evaluation against liver cancer cell lines, J. Taibah Univ. Sci. 16 (1) (2022) 1005–1015, https://doi.org/10.1080/16583655.2022.2135805.

[43] V. Kamat, R. Santosh, B. Poojary, S.P. Nayak, B.K. Kumar, M. Faheem Sankaranarayanan, S. Khanapure, D. Avilla Barretto, S.K. Vootla, Pyridine- and thiazole-based Hydrazides with promising anti-inflammatory and antimicrobial activities along with their *in silico* studies, ACS Omega 5 (39) (2020) 25228–25239, https://doi.org/10.1021/acsomega.0c03386.

[44] J.D. Bilavendran, A. Manikandan, Thangarasu Pandiyan, K.K. Sivakumar, Synthesis and discovery of Pyrazolo-pyridine Analogs as inflammation medications through Pro- and anti-inflammatory Cytokine and COX-2 inhibition assessments, Bioorg. Chem. 94 (2020) 103484, https://doi.org/10.1016/j.bioorg.2019.103484.

[45] M.H. Ali Eslam, M.S. Abdel-Maksoud, R.M. Hassan, K.I. Mersal, U.M. Ammar, S. Choi, H. He-Soo, B.-H. Jeong, A. Lee, K.-T. Lee, C.-H. Oh, Design, synthesis and anti-inflammatory activity of Imidazole-5-yl pyridine derivatives as P38α/MAPK14 inhibitor, Bioorg. Med. Chem. 31 (2021) 115969, https://doi.org/10.1016/j.bmc.2020.115969.

[46] I.T. Chaban, V.V. Ogurtsov, V.S. Matiychuk, I.G. Chaban, I.L. Demchuk, I.A. Nektegayev, I. Ynthesis, Anti-inflammatory and antioxidant activities of novel 3H-Thiazolo[4,5-b]Pyridines, Acta Chim. Slov. 66 (1) (2019) 103–111, https://doi.org/10.17344/acsi.2018.4570.

[47] Y.M. Omar, H.H.M. Abdu-Allah, S.G. Abdel-Moty, Synthesis, biological evaluation and docking study of 1,3,4-thiadiazole-Thiazolidinone hybrids as anti-inflammatory agents with dual inhibition of COX-2 and 15-LOX, Bioorg. Chem. 80 (2018) 461–471, https://doi.org/10.1016/j.bioorg.2018.06.036.

[48] A. Cristina, D. Leonte, L. Vlase, L. Bencze, S. Imre, G. Marc, B. Apan, C. Mogoşan, V. Zaharia, Heterocycles 48. Synthesis, characterization and biological evaluation of Imidazo[2,1-b][1,3,4]Thiadiazole derivatives as anti-inflammatory agents, Molecules 23 (10) (2018) 2425, https://doi.org/10.3390/molecules23102425.

[49] Y.M. Omar, S.G. Abdel-Moty, Hajjaj H.M. Abdu-Allah, Further insight into the dual COX-2 and 15-LOX anti-inflammatory activity of 1,3,4-thiadiazole-Thiazolidinone hybrids: the contribution of the substituents at 5th positions is size Dependent, Bioorg. Chem. 97 (2020) 103657, https://doi.org/10.1016/j.bioorg.2020.103657.

[50] J. Frank, Villani and mary S. King. 3-benzoylpyridine, Org. Synth. 37 (6) (1957), https://doi.org/10.15227/orgsyn.037.0006.

[51] M.A. Said, S.M. Riyadh, N.S. Al-Kaff, A.A. Nayl, K.D. Khalil, S. Bräse, S.M. Gomha, Synthesis and greener pastures biological study of bis-thiadiazoles as potential Covid-19 drug candidates, Arab. J. Chem. 15 (9) (2022) 104101, https://doi.org/10.1016/j.arabjc.2022.104101.

[52] A.S. Abouzied, J.Y. Al-Humaidi, A.S. Bazaid, H. Qanash, N.K. Binsaleh, A. Alamri, S.M. Gomha, Synthesis, molecular docking study, and cytotoxicity evaluation of some novel 1, 3, 4-thiadiazole as well as 1, 3-thiazole derivatives bearing a pyridine moiety, Molecules 27 (19) (2022) 6368, https://doi.org/10.3390/molecules27196368.

[53] S. Firdausiah, S.A. Hasbullah, B.M. Yamin, Synthesis, Structurale elucidation and antioxidant study of Ortho -substituted N, N'-Bis(Benzamidothiocarbonyl) Hydrazine derivatives, in: Journal of Physics: Conference Series, 2018 12010, https://doi.org/10.1088/1742-6596/979/1/012010, 979.

[54] K.P. Harish, K.N. Mohana, L. Mallesha, Synthesis of Pyrazine substituted 1,3,4-thiadiazole derivatives and their Anticonvulsant activity, Organic Chemistry International 2013 (2013) 1–8, https://doi.org/10.1155/2013/631723.

[55] S. Zhu, J. Li, A novel synthesis of isothiocyanates from amines and phenyl isothiocyanate *via* replacement reaction, Organic Chemistry International 75 (9) (2021) 4543–4547, https://doi.org/10.1007/s11696-021-01692-x.

[56] R. Roll, T. Höfer-Bosse, D. Kayser, New perspectives in acute toxicity testing of chemicals, Toxicol Lett Suppl 31 (1986) 86.

[57] R. Roll, M. Riebschlaeger, U. Mischke, D. Kayser, New approaches to acute toxicity testing of chemicals, Federal Health Gazette (FR Germany) 32 (8) (1989).

[58] C.A. Winter, E.A. Risley, G.W. Nuss, Carrageenin-induced edema in Hind paw of the rat as an Assay for Antiinflammatory drugs, Exp. Biol. Med. 111 (3) (1962) 544–547, https://doi.org/10.3181/00379727-111-27849.

[59] J.S. Bang, D.H. Oh, H.M. Choi, B.-J. Sur, S.-J. Lim, J.Y. Kim, H.-I. Yang, M.C. Yoo, D.-H. Hahm, K.S. Kim, Anti-inflammatory and Antiarthritic effects of Piperine in Human Interleukin 1β-Stimulated Fibroblast-like Synoviocytes and in rat arthritis models, Arthritis Res. Ther. 11 (2) (2009) R49, https://doi.org/10.1186/ar2662.

[60] S. Alqasoumi, G. Abd, E. Soliman, A. Awaad, A. El, R.M. Donia, S. Bin, Anti-inflammatory activity, safety and protective effects of Leptadenia pyrotechnica, Haloxylon salicornicum and Ochradenus baccatus in ulcerative colitis, Phytopharmacology 2 (1) (2012) 58–71. https://api.semanticscholar.org/CorpusID:20118180.

[61] J.N. Sharma, A.M. Samud, M.Z. Asmawi, Comparison between plethysmometer and Micrometer methods to measure acute paw Oedema for screening anti-inflammatory activity in Mice, Inflammopharmacology 12 (1) (2004) 89–94, https://doi.org/10.1163/156856004773121400.

[62] V.B. Owoyele, J.O. Adediji, A.O. Soladoye, Anti-inflammatory activity of Aqueous Leaf Extract of ChromolaenaOdorata, Inflammopharmacology 13 (5–6) (2005) 479–484, https://doi.org/10.1163/156856005774649386.

[63] S.K. Konidala, V. Kotra, R.C.S.R. Danduga, P.K. Kola, Coumarin-chalcone hybrids targeting Insulin receptor: design, synthesis, anti-Diabetic activity, and molecular docking, Bioorganic Chemisty 104 (2020) 104207, https://doi.org/10.1016/j.bioorg.2020.104207.

[64] A.K. Subramani, A. Sivaperuman, R. Natarajan, R.R. Bhandare, A.B. Shaik, QSAR and molecular docking studies of pyrimidine-Coumarin-Triazole conjugates as prospective anti-Breast cancer agents, Molecules 27 (6) (2022) 1845, https://doi.org/10.3390/molecules27061845.

[65] Babu Lagu Surendra, Rajendra Prasad Yejella, Srinath Nissankararao, R.R. Bhandare, V. Sampath, Bontha Venkata Subrahmanya Lokesh, Md Abdur Rahman, A. B. Shaik, Antitubercular activity assessment of Fluorinated Chalcones, 2-Aminopyridine-3-Carbonitrile and 2-amino-4H-Pyran-3-Carbonitrile derivatives: *In vitro*, molecular docking and in-silico drug Likeliness studies, PLoS One 17 (6) (2022) e0265068, https://doi.org/10.1371/journal.pone.0265068.

[66] Schrödinger Release 2022-1: Desmond Molecular Dynamics System, D. E. Shaw Research, New York, NY, 2021, Maestro-Desmond Interoperability Tools, Schrödinger, New York, NY, 2021.

[67] H.M. Berman, The protein Data Bank, Nucleic Acids Res. 28 (1) (2000) 235–242, https://doi.org/10.1093/nar/28.1.235.
[68] J. Gelpi, A. Hospital, R. Goñi, M. Orozco, Molecular dynamics simulations: Advances and applications, Comput. Biol. Chem. Adv. Appl. 37 (2015), https://doi.org/10.2147/AABC.S70333.
[69] P. Mark, L. Nilsson, Structure and dynamics of the TIP3P, SPC, and SPC/E water models at 298 K, J. Phys. Chem. 105 (43) (2001) 9954–9960, https://doi.org/10.1021/jp003020w.
[70] W.L. Jorgensen, D.S. Maxwell, J. Tirado-Rives, Development and testing of the OPLS all-atom force field on conformational Energetics and properties of Organic Liquids, J. Am. Chem. Soc. 118 (45) (1996) 11225–11236, https://doi.org/10.1021/ja9621760.
[71] M. Tuckerman, B.J. Berne, G.J. Martyna, Reversible multiple time scale molecular dynamics, J. Chem. Phys. 97 (3) (1992) 1990–2001, https://doi.org/10.1063/1.463137.
[72] A. Cheng, K.M. Merz, Application of the Nosé−Hoover chain algorithm to the study of protein dynamics, J. Phys. Chem. 100 (5) (1996) 1927–1937, https://doi.org/10.1021/jp951968y.
[73] G. Kalibaeva, M. Ferrario, G. Ciccotti, Constant pressure-constant temperature molecular dynamics: a Correct Constrained NPT ensemble using the molecular Virial, Molicural Physics 101 (6) (2003) 765–778, https://doi.org/10.1080/0026897021000044025.
[74] R. Chinnasamy, R. Sundararajan, S. Govindaraj, Synthesis, characterization, and analgesic activity of novel Schiff base of Isatin derivatives, \"J. Adv. Pharm. Technol. Research\"\" (JAPTR)\" 1 (3) (2010) 342, https://doi.org/10.4103/0110-5558.72428.
[75] M.M. Ibrahim, T. Elsaman, Al Nour, M.Y. Synthesis, Anti-inflammatory activity, and *In silico* study of novel diclofenac and Isatin conjugates, International Journal of Medicinal Chemistry 2018 (2018) 1–11, https://doi.org/10.1155/2018/9139786.
[76] A. Redzicka, Ż. Czyżnikowska, B. Wiatrak, K. Gębczak, A. Kochel, Design and synthesis of N-substituted 3,4-Pyrroledicarboximides as potential anti-inflammatory agents, Int. J. Mol. Sci. 22 (3) (2021) 1410, https://doi.org/10.3390/ijms22031410.
[77] J.P. Soni, D.J. Sen, K.M. Modh, Structure activity relationship studies of synthesised pyrazolone derivatives of imidazole, benzimidazole and benztriazole moiety for anti-inflammatory activity, J. Appl. Pharmaceut. Sci. 1 (4) (2011) 115–120.
[78] R. Veerasamy, A. Roy, R. Karunakaran, H. Rajak, Structure–activity relationship analysis of Benzimidazoles as emerging anti-inflammatory agents: an overview, Pharmaceuticals 14 (7) (2021) 663, https://doi.org/10.3390/ph14070663.
[79] M.A. Sultan, M.S. Galil, M. Al-Qubati, M.M. Omar, A. Barakat, Synthesis, molecular docking, drug likeness analysis, and ADMET prediction of the chlorinated ethano anthracene derivatives as possible antidepressant agents, Appl. Sci. 10 (21) (2020) 7727.
[80] C.Y. Jia, J.Y. Li, G.F. Hao, G.F. Yang, A drug-likeness toolbox facilitates ADMET study in drug discovery, Drug Discov. Today 25 (1) (2020) 248–258, https://doi.org/10.1016/j.drudis.2019.10.014.
[81] B. Bakchi, A.D. Krishna, E. Sreecharan, V.B.J. Ganesh, M. Niharika, S. Maharshi, A.B. Shaik, An overview on applications of SwissADME web tool in the design and development of anticancer, antitubercular and antimicrobial agents: a medicinal chemist's perspective, J. Mol. Struct. 1259 (2022) 132712, https://doi.org/10.1016/j.molstruc.2022.132712.
[82] A. Daina, O. Michielin, V. Zoete, SwissADME: a free web tool to evaluate pharmacokinetics, drug-likeness and medicinal chemistry friendliness of small molecules, Sci. Rep. 7 (2017) 42717, https://doi.org/10.1038/srep42717.